Journal of Hazardous Materials 162 (2009) 716–723

Contents lists available at ScienceDirect

Journal of Hazardous Materials

journal homepage: www.elsevier.com/locate/jhazmat

Photodegradation of polycyclic aromatic hydrocarbon pyrene by iron oxide in solid phase

Y. Wang[a,b], C.S. Liu[a], F.B. Li[a,*], C.P. Liu[a], J.B. Liang[b]

[a] *Guangdong Key Laboratory of Agricultural Environment Pollution Integrated Control, Guangdong Institute of Eco-Environmental and Soil Sciences, Guangzhou 510650, PR China*
[b] *Institute of Bioscience, University Putra Malaysia, 43400 UPM, Serdang, Selangor, Malaysia*

ARTICLE INFO

Article history:
Received 16 February 2008
Received in revised form 20 May 2008
Accepted 20 May 2008
Available online 23 May 2008

Keywords:
Photodegradation
PAH
Pyrene
Iron oxide
Solid phase

ABSTRACT

To better understand the photodegradation of polycyclic aromatic hydrocarbons (PAH) in solid phase in natural environment, laboratory experiments were conducted to study the influencing factors, kinetics and intermediate compound of pyrene photodegradation by iron oxides. The results showed that the pyrene photodegradation rate followed the order of α-FeOOH > α-Fe_2O_3 > γ-Fe_2O_3 > γ-FeOOH at the same reaction conditions. Lower dosage of α-FeOOH and higher light intensity increased the photodegradation rate of pyrene. Iron oxides and oxalic acid can set up a photo-Fenton-like system without additional H_2O_2 in solid phase to enhance the photodegradation of pyrene under UV irradiation. All reaction followed the first-order reaction kinetics. The half-life ($t_{1/2}$) of pyrene in the system showed the higher efficiencies of using iron oxide as photocatalyst to degrade pyrene. Intermediate compound pyreno was found during photodegradation reactions by gas chromatography–mass spectrometry (GC–MS). The photodegradation efficiency for PAHs in this photo-Fenton-like system was also confirmed by using the contaminated soil samples. This work provides some useful information to understand the remediation of PAHs contaminated soils by photochemical techniques under practical condition.

1. Introduction

Polycyclic aromatic hydrocarbons (PAHs) are pollutants produced via natural and anthropogenic sources, generated during the incomplete combustion of solid and liquid fuels or derived from industrial activities. They are ubiquitous pollutants that occur in natural phase such as soil, sediment, water and air, and are harmful to environment and health of human being due to their high degree of mutagenicity and carcinogenicity when they enter the human body [1–3]. A total of 16 PAHs were included in the European Union (EU) and the United States Environmental Protection Agency (US EPA) priority pollutants list. Investigating the progress of PAHs degradation in the environment, and developing efficient and economical degradation technologies for PAH is an important research needed.

Many studies have been conducted on biodegradation of individual PAHs and related compounds [4–8]. And some limitations have been presented, such as long degradation periods and the difficulty of condition controlled. Furthermore, some heavier PAHs (with more than 3 rings) are difficult to be biodegraded due to their poor water-solubility [3,9,10]. Recently, chemical technologies for PAHs degradation have been paid much attention, and among which the photodegradation has been given much emphasis [11]. Environmental applications of heterogeneous photocatalysis, especially using titanium dioxide (TiO_2) have been extensively investigated to remove PAHs in aqueous solution [12–14]. Since PAHs have extremely low solubility in water, the studies mentioned above had to use organic solvent to dissolve PAHs or use surfactants to increase the solubility of PAHs [15], which might cause difficulty in samples analyses and thus the study of degradation of PAHs because of the existence of the organic matters accompanied in PAHs [16]. Normally PAHs are presented in much higher concentrations in soil phase than in aqueous phase. To date, although there were few studies reporting the degradation of PAHs in solid phase without disturbance from the organic solvent and surfactants [17,18], limited studies had been reported on the influencing factors and intermediate products during photodegradation by iron oxide in solid phase.

Iron oxides are natural minerals found in soils and rocks, lakes and rivers, on the seafloor, in air and organism [19]. Major iron oxides include goethite (α-FeOOH), hematite (α-Fe_2O_3), lepidocrocite (γ-FeOOH), and maghemite (γ-Fe_2O_3). Iron oxides can act as natural photo catalysts to catalyze degradation of organic pollutants in environment [20,21]. It has also been reported that

* Corresponding author. Tel.: +86 20 87024721; fax: +86 20 87024123.
E-mail addresses: cefbli@soil.gd.cn, cefbli@hotmail.com (F.B. Li).

0304-3894/$ – see front matter © 2008 Elsevier B.V. All rights reserved.
doi:10.1016/j.jhazmat.2008.05.086

iron oxide and oxalic acid, a polycarboxylic acid has strong chelating ability with multivalent cations, mainly exuded by plants in natural environment [22], can set up a Fenton-like system without additional H_2O_2 to photodegrade organic pollutants in aqueous solutions [23,24].

In this study, the experiments were conducted to investigate the photocatalytic degradation by iron oxides on solid phase pyrene, a PAH with the molecular formula of $C_{16}H_{10}$ and the molecular weight of 202.3. In order to further understand the degradation of pyrene by iron oxides, the influencing factors, including dosage of iron oxide, type of the iron oxide, and the UV light intensity were also studied. Furthermore, the experiments of dependence on initial concentration of oxalic acid were conducted to evaluate the photochemical activities of the Fenton-like system and the effect of oxalic acid on the degradation of pyrene by the iron oxide–oxalic acid system. The intermediate compound was also studied by using GC–MS. And contaminated soils had been sampled to evaluate the photodegradation efficiency of PAHs by Fenton-like system.

2. Materials and methods

2.1. Chemicals

Pyrene (analytical grade) was purchased from Janssen Chimica (Belgium). A pyrene stock solution was prepared at the concentration of 100 mg/L and then diluted into the designated concentration standards in mobile phase to construct a calibration curve. Methanol and methylene dichloride of HPLC grade and distilled water were used in this experiment, and the glassware used were dipped in chromic acid cleaning mixture for 6 h, and then rinsed with distilled water before being dried at 110 °C for 8 h.

2.2. Preparation and characterization of iron oxides

γ-FeOOH (color of orange) was prepared by hydrothermal method [25], and α-Fe_2O_3 (red) was formed by sintering γ-FeOOH powder at 420 °C for 2 h at a programmed heating rate of 2 °C/min [26]. α-FeOOH (yellow-brown) was prepared as reported by Schwertmamm and Cornell [19] while γ-Fe_2O_3 was prepared with the following procedure: Firstly, dissolving 16 g of $FeCl_2{\cdot}4H_2O$, 22.4 g of $(CH_2)_6N_4$, and 5.6 g of $NaNO_3$ in 400, 80, and 80 mL double-distilled water, respectively. The three solutions were mixed to obtain a bluish green precipitate which was later aged in the mixture at 80 °C for 6 h prior to centrifugation. The precipitate was washed three times with alcohol and distilled water to remove anions and organic impurities before dried at 65 °C for 48 h. After ground to pass through 100 mesh screens, the dark red-brown γ-Fe_2O_3 powders were obtained.

The X-ray powder diffraction patterns of iron oxides were recorded on a Rigaku D/Max-III. A diffract meter at room temperature, operating at 30 kV and 30 mA, using a Cu Kα radiation (λ = 0.15418 nm). The phases were identified by comparing diffraction patterns with those on the standard powder XRD cards compiled by the Joint Committee on Powder Diffraction Standards (JCPDS) [27]. The total surface area and total pore volume of four samples were measured by the Brunauer–Emmett–Teller (BET) method in which the N_2 adsorption at 77 K was applied and Carlo Erba Sorptometer was used [28,29].

2.3. Pyrene photodegradation experiments

2.3.1. Experimental process

Photodegradation of pyrene were carried out in a Pyrex quadrate photoreactor, in which 8 black light lamps with a power of 48 W (Nanjing Ziguang, China) with the main emission at 365 nm were positioned equably. The photoreactor was sealed with window blind to avoid indoor light irradiation and the temperature was controlled by the air-conditioning during reaction.

The reaction mixture was produced by adding 4 mL of 10 mg/L pyrene–methylene dichloride solution into 2 g iron oxide. Prior to photoreaction, the suspension was added with 10 mL of the methylene dichloride and magnetically stirred in the dark for 12 h in aerator to establish adsorption/desorption equilibrium and also to volatilize the methylene dichloride. Each 0.2 g of the dried reaction mixture was screened (100 mesh) evenly onto an optical glass (10 cm × 10 cm) and which was later covered by another optical glass. Six pairs of optical glasses were prepared for every kinetic experiment. The weight of reaction mixture after screening was determined and was found to be near identical with an average weight of 0.1991 g (ranged from 0.1984 to 0.2001). During the photoreaction process, the prepared optical glasses were placed under the UV light. And at the given time intervals, the samples were collected from a pair of optical glasses, and then extracted and analyzed as soon as possible.

2.3.2. Extraction and analysis of pyrene

After diverted to 50 mL centrifugal tubes, the samples were immediately added with 10 mL methylene dichloride. The centrifugal tubes were covered by tinfoil to prevent the light irrigation. The mixtures were extracted for 30 min in an ultrasonic bath extractor at the controlled temperature below 10 °C by using ice. After extraction, the extract was immediately passed through a 0.45 μm organic filter paper. The same extraction process was repeated twice. The effluent samples were collected and stored for later analysis.

Pyrene was determined by high performance liquid chromatography (HPLC) consisted of a Waters 1525 binary pump, a Waters 2487 dual λ Absorbance UV/vis detector at 254 nm and a reversed-phase column of 5 μm Symmetry-C18, 4.6 mm i.d. × 25 cm long (Waters, USA). The methanol-ultrapure water mixture (90:10) was used at mobile flow rate of 1.0 mL/min under isocratic conditions at room temperature. Samples of 20 μL were injected into the column through the sample loop for analysis. The data was processed with the Breeze software. And the relative standard deviation for HPLC analysis was controlled within 2%.

2.3.3. Experimental design

This study consisted of four experiments (Table 1). The first was conducted to examine the effects of type of iron oxides. 2 g of four types of iron oxide, namely goethite (α-FeOOH), hematite (α-Fe_2O_3), maghemite (γ-Fe_2O_3) and lepidocrocite (γ-FeOOH) were used. To investigate the effect of the dosages of iron oxide, the second experiment was carried out by adding 4 mL of 10 mg/L pyrene into 0.05, 0.1, 0.2 and 0.5 g α-FeOOH, respectively, to obtain 5, 10, 20, 50 g/m^2 α-FeOOH in reaction optical glass. To examine the effects of initial oxalic acid concentrations, the third experiment was conducted by adding oxalic acid to 4 mL of 10 mg/L pyrene and 2 g α-FeOOH mixture to achieve 0, 0.22, 0.45, 0.9 and 1.34 oxalate and goethite ratio. To investigate the effect of light intensities, the last experiment was conducted by irradiating 4 mL of 10 mg/L Pyrene and 2 g α-FeOOH mixture using different lamps with intensity of 480, 2400 and 4800 μW/cm^2, respectively. All experiments in the study were replicated three times.

2.3.4. Recovery and blank experiments

In order to verify the efficiency of sample extraction, recovery experiments were performed. Pyrene–methylene dichloride solution was added to 0.2 g of α-FeOOH to obtain pyrene concentrations of 5, 10, 15, 20 and 25 mg/kg. The samples, including the blank (without pyrene) were analyzed by the procedure described in

Table 1
Experimental design for the four set of experiments

Experiment	Type of iron oxide	Oxides dosage (g/m^2)	Molar ratio of oxalate and iron oxide	Intensity of UV light ($\mu w/cm^2$)
1	α-FeOOH, α-Fe_2O_3, γ-FeOOH, γ-Fe_2O_3	20	0	480
2	α-FeOOH	5, 10, 20, 50	0	480
3	α-FeOOH	20	0, 0.22, 0.45, 0.90, 1.34	480
4	α-FeOOH	20	0	480, 2400, 4800

Section 2.3.2. The recovery and blank experiments were repeated five times.

The recovery of the pyrene increased from 61% for 5 mg pyrene/kg α-FeOOH to 74% for 25 mg pyrene/kg α-FeOOH (Table 2). The recovery rates appeared to be relatively low, but similar results were reported by other groups [9,30,31]. The standard deviations of each dosage (5 replicates) were low (Table 2), and, therefore, the recovery rate reported in this study indicates that the analytical method used is reliable. The absence of Pyrene in the blank samples confirmed that pyrene in the α-FeOOH samples was derived from our factitious inclusion. The recoveries exhibited close relationship with pyrene concentrations ($R^2 = 0.9496$). Data presented in this study are corrected accordingly using the formula: $x = 47.66 \times [(1 + 0.071z)^{0.5} - 1]$ derived from the following calculation:

$$y = 0.62x + 59.1$$

and,

$$y = \frac{z}{x} \times 100$$

therefore,

$$62x + 5910 = \frac{z}{x} \times 10000, \quad x = 47.66 \times \left[(1 + 0.071z)^{0.5} - 1\right]$$

In this study, z ranged from 0 to 20, therefore,

$$x = 47.66 \times \left[(1 + 0.071z)^{0.5} - 1\right]$$

where y = recovery (%); x = added concentration of pyrene in α-FeOOH (mg/kg); z = detectable pyrene concentration from experiment (mg/kg).

2.4. The contaminated soil experiment

2.4.1. The contaminated soil used in the experiments

The PAHs contaminated soils were collected from Dazhen village, Nanhai district, Foshan city of South China (latitude 23.08656°N and longitude 113.10952°E). The sampled red soil had been used for vegetable production. The sampling depth was 0–20 cm with Fe_2O_3 concentration of 67.83 g/kg. Prior to the experiments, the soil was dried naturally under shade and ground to pass through with 200 mesh screen. This soil was contaminated primarily by 9 PAHs, namely Fluoranthene, Pyrene, Benzo[*a*]anthracene, Chrysene, Benzo[*b*]fluoranthene, Benzo[*k*]fluoranthene, Benzo[*a*]pyrene, Indeno[1,2,3-*cd*]pyrene and Benzo[*ghi*]perylene, with their corresponding concentrations of 0.7147, 0.4823, 0.1952, 0.3532, 0.3977, 0.0927, 0.1586, 0.1814 and 0.1939 mg/kg, respectively.

Table 2
Recovery and blank concentration of pyrene in iron oxide

Concentration of pyrene in α-FeOOH (mg/kg)	Recovery (%)	Blank (mg/kg)
5	61 ± 1.15	n.d.
10	67 ± 1.08	0.001
15	68 ± 2.13	0.001
20	72 ± 0.84	n.d.
25	74 ± 0.91	n.d.

2.4.2. Analysis of pyrene photodegradation intermediate products and PAHs in contaminated soil

The extraction of pyrene photodegradation intermediate product and PAHs in contaminated soil was as described in Section 2.3.2 were analyzed by gas chromatography coupled with mass spectrometry (GC–MS, DSQ Thermo, USA). The recovery of the samples was assessed by response factor method combined with internal standard method, and adjusted, using a microsyringe, to an exact volume before injection for the calculation of the injected concentration. The recovery of surrogates was 84 and 92% for Phenanthrene-D10 and Chrysene-D12, respectively. Comparing to the mentioned before experiment, the recoveries significantly increased. This case could be due to the difference in pyrene adsorption in different particles matrix [32]. The GC instrument was equipped with split/splitless injector and a TR-5MS column was used for separation (30 m, 0.25 mm i.d., 0.25 μm film thickness). The initial temperature was set at 60 °C and was held for 1 min in splitless mode. When the splitter was opened, the oven was heated to 240 °C with a heating rate of 8 °C/min, and then to 260 °C with a rate of 2 °C/min after maintained for 5 min. The solvent delay time was set for 4 min while the temperature of the transfer line was set at 250 °C. Mass spectra were recorded at 3 scans/s under electron impact of 70 eV at the mass range of 50–350 amu.

3. Results and discussion

3.1. Properties of iron oxides

The X-ray diffractograms (XRD) of the prepared iron oxides are shown in Fig. 1. Pure γ-FeOOH powder was obtained because the 8

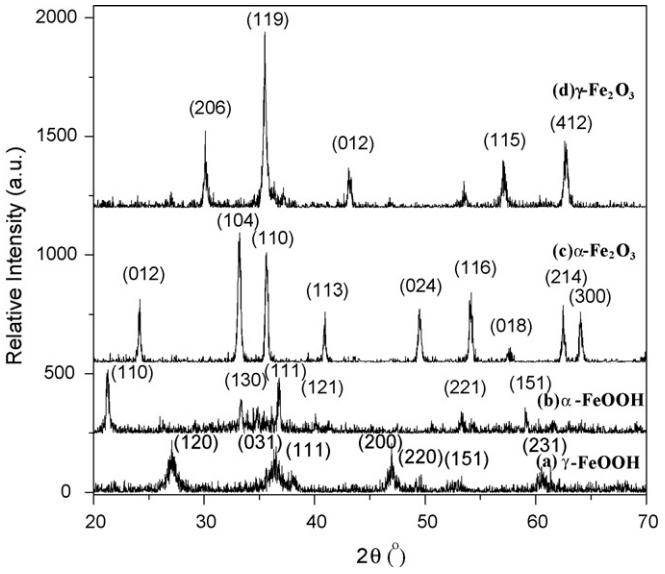

Fig. 1. The XRD graphs of iron oxides powders.

peaks (Fig. 1a) were in accordance to the characteristic peaks of γ-FeOOH [27]. Similarly pure α-FeOOH with peaks (Fig. 1b) of (1 1 0), (1 3 0), (1 1 1), (1 2 1), (2 2 1), and (1 5 1), α-Fe_2O_3 with the characteristic peaks (Fig. 1c) of (0 1 2), (1 0 4), (1 1 0), (1 1 3), (0 2 4), (1 1 6), (2 1 4) and (3 0 0), and γ-Fe_2O_3 with peaks (Fig. 1d) of (2 2 0), (3 1 1), (2 2 2), (4 0 0), (4 2 2), (5 1 1) and (4 4 0) were obtained. The crystal sizes of γ-Fe_2O_3, γ-FeOOH, α-Fe_2O_3 and α-FeOOH were 43.2, 13.7, 54.7 and 41.9 nm, respectively, which were deduced from Sherrer's formula with the corresponding strongest XRD peak. The specific surface areas measured by BET-BJH method were 14.36, 115.44, 29.40 and 120.93 m^2/g and the total pore volumes were 0.05, 0.30, 0.27 and 0.16 cm^3/g for γ-Fe_2O_3, γ-FeOOH, α-Fe_2O_3 and α-FeOOH, respectively.

3.2. Dependence of pyrene photodegradation on type of iron oxides

Fig. 2 showed the photodegradation of pyrene with the initial concentration of 20 mg/kg under UV irradiation of 480 μW/cm^2 on different iron oxides. The results indicated that all the four iron oxides had high photocatalytic activities and pyrene can be efficiently degraded by them under UV light irradiation. The photocatalytic degradation of pyrene followed the first-order reaction kinetics with the first-order kinetics constants (k) for pyrene degradation as 0.2301 (R = 0.984), 0.1864 (R = 0.984), 0.2084 (R = 0.984) and 0.1829 h^{-1} (R = 0.999) when it was degraded by α-FeOOH, γ-FeOOH, α-Fe_2O_3 and γ-Fe_2O_3, respectively (Table 3). The half lives ($t_{1/2}$) of pyrene degraded by α-FeOOH, γ-FeOOH, α-Fe_2O_3 and γ-Fe_2O_3 were 3.01, 3.72, 3.33 and 3.79 h, respectively. Niu et al. [33] had reported that the $t_{1/2}$ for pyrene on needle surfaces with no direct sunlight irradiation was 33 h. In this study, the $t_{1/2}$ of pyrene degradation by iron oxides under UV irradiation were much shorter than 33 h, indicating that in solid phase, iron oxides have high photocatalytic activities and can degrade pyrene efficiently. The results also showed that the photodegradation rate of pyrene on α-FeOOH was the highest with the k value of 0.2301 h^{-1}, presumably due to the higher photocatalytic activity of α-FeOOH because of its basic morphology-acicular crystal structure [34].

Table 3
The k values during the four set of experiments

Peptizing conditions	Pyrene	
	k (h^{-1})	R
Dosage of iron oxide (g)		
0.05	0.2571 ± 0.0252	0.918
0.10	0.2369 ± 0.0168	0.966
0.20	0.2301 ± 0.0117	0.984
0.50	0.1694 ± 0.0126	0.960
Light intensity (μW/cm^2)		
410	0.2301 ± 0.0117	0.984
2800	0.2390 ± 0.0109	0.984
4810	0.2695 ± 0.0227	0.948
Type of iron oxide		
α-FeOOH	0.2301 ± 0.0112	0.984
γ-FeOOH	0.1864 ± 0.0087	0.984
α-Fe_2O_3	0.2084 ± 0.0105	0.984
γ-Fe_2O_3	0.1829 ± 0.0024	0.999
Initial concentration of oxalic acid (mmol/L)		
0	0.2301 ± 0.0117	0.984
0.5	0.2643 ± 0.0053	0.997
1.0	0.2676 ± 0.0102	0.993
2.0	0.2920 ± 0.0135	0.987
3.0	0.4424 ± 0.0223	0.985

3.3. Effect of the dosages of α-FeOOH with the constant reaction surface area

Fig. 3 showed the effect of the α-FeOOH dosages with the constant reaction surface area on the photodegradation of pyrene with the initial concentration of 20 mg/kg under UV irradiation of 480 μW/cm^2. It can be seen that photodegradation rate of pyrene was inversely related to the dosages of α-FeOOH. When the dosages of α-FeOOH were 5, 10, 20 and 50 g/m^2, the first-order kinetics constants k for pyrene degradation were 0.2571 (R = 0.918), 0.2369 (R = 0.966), 0.2301 (R = 0.984) and 0.1694 (R = 0.960) h^{-1} (Table 3). With the same initial pyrene concentration, the photodegradation rate of pyrene obviously decreased with increased dosage of α-FeOOH. The UV light intensity was important in the photocatalytic degradation process, especially in the solid phase degradation as studied here. When increasing the dosage of iron oxides,

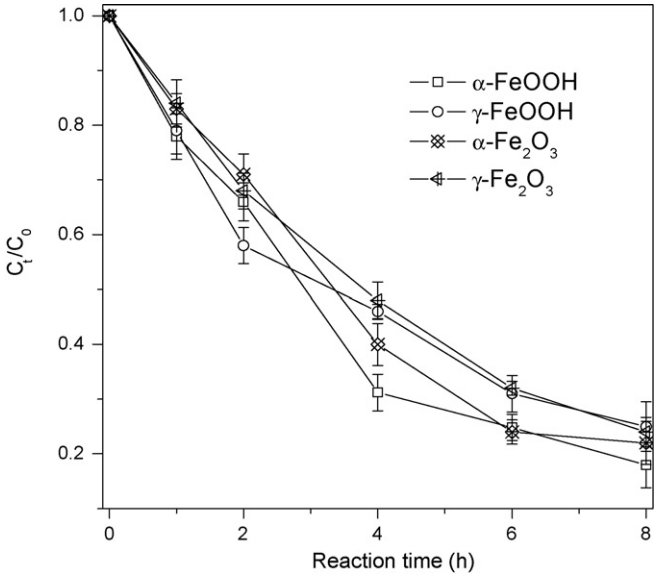

Fig. 2. The effect of the type of iron oxide with the dosage of 20 g/m^2 on the photodegradation of pyrene with the initial concentration of 20 mg/kg under 480 μW/cm^2 UV irradiation.

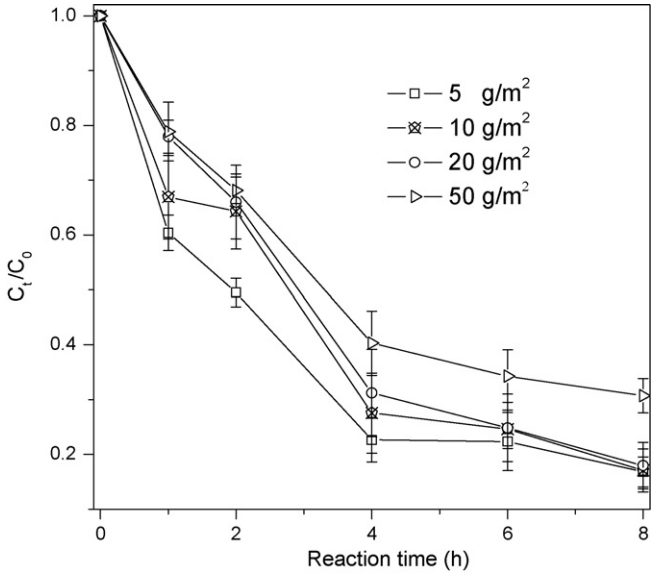

Fig. 3. The effect of the α-FeOOH dosage on the photodegradation of pyrene with the initial concentration of 20 mg/kg under 480 μW/cm^2 UV irradiation.

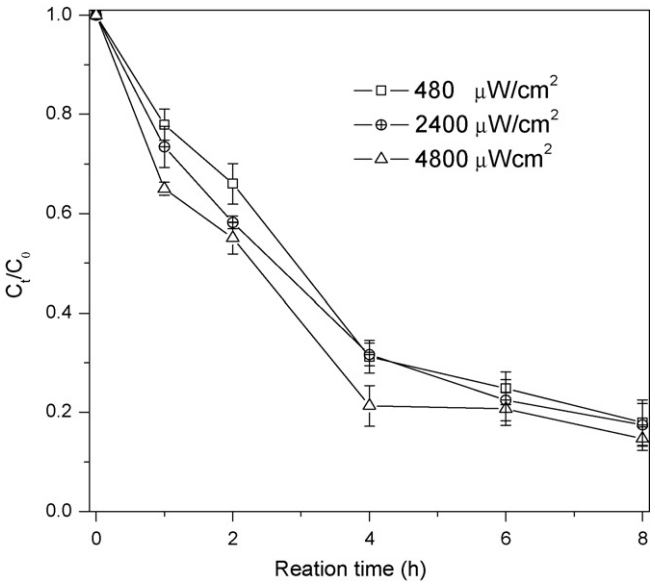

Fig. 4. The effect of the intensity of UV irradiation on the photodegradation of pyrene with the initial concentration of 20 mg/kg by using 20 g/m^2 α-FeOOH.

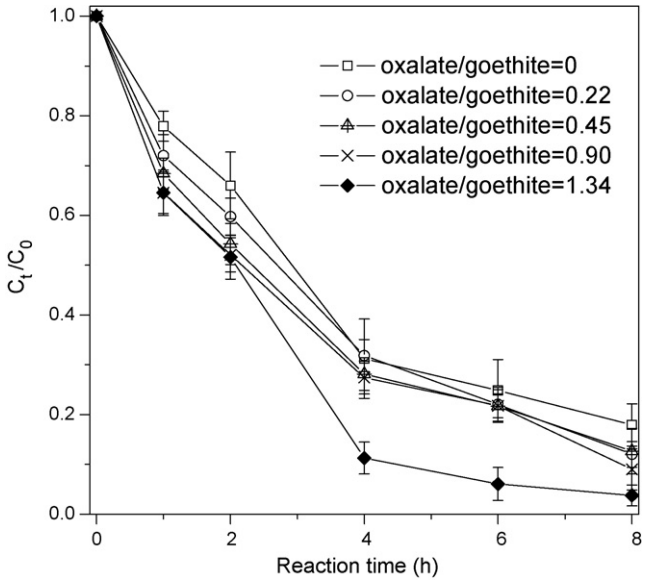

Fig. 5. The effect of the molar ratio of oxalate and goethite on the photodegradation of pyrene with the initial concentration of 20 mg/kg under 480 μW/cm^2 UV irradiation by using 20 g/m^2 α-FeOOH.

the thickness of iron oxides on the same optical glass would increase. Since the intensity of UV light decays rapidly in the solid phase, the UV light utilization rate would decrease with an increased dosage of iron oxide for pyrene degradation. As a result, when the dosage of iron oxide increased, pyrene degradation rate decreased.

3.4. Effect of the light intensities

It is well established that the light intensity is an important factor affecting photocatalytic degradation of pyrene. Fig. 4 showed the effect of the light intensity on the photodegradation of pyrene with the initial concentration of 20 mg/kg by 20 g/m^2 α-FeOOH. The results showed that pyrene degradation rates increased slightly with the significant increase in light intensity. When the irradiating light intensities increased from 480 to 2800 and 4800 μW/cm^2, the k values for pyrene degradation increased from 0.2301 (R = 0.984) to 0.2390 (R = 0.984) and 0.2695 (R = 0.948) h^{-1}, respectively (Table 3). Guo et al. [35] reported that light intensity strongly influence the PAH degradation in gaseous phase. However, in this study, the percentage of pyrene degradation increased from 34 to 45% when the light intensities increased 10 times from 480 μW/cm^2 after 6 h reaction. The case should be attributable to the obstruction in the penetration of UV light in the solid phase [36].

3.5. Effect of the initial concentration of oxalic acid

Fig. 5 showed the effect of the molar ratio of oxalate and goethite on the photodegradation of pyrene with the initial concentration of 20 mg/kg and light intensity of 480 μW/cm^2 by using 20 g/m^2 α-FeOOH. It can be seen that oxalic acid had obvious effect on pyrene degradation. In the absence of oxalic acid in the solid phase, pyrene degraded at the rate (k) of 0.2301 h^{-1}. When the molar ratio of oxalate and goethite was up to 0.22, 0.45, 0.90 and 1.34, respectively, the k values of pyrene degradation increased to 0.2643, 0.2676, 0.2920 and 0.4424 h^{-1}, respectively (Table 3). In the absence of oxalic acid, iron oxides act as a photocatalyst, while in the presence of oxalic acid, the so called Fenton-like system, an iron oxide–oxalate system, was initiated and further speeded up the degradation of organic pollutants [37]. The present results confirmed that in combination with oxalate, the photodegradation of pyrene by iron oxides was greatly accelerated.

However, our previous investigation reported that excessive oxalate would occupy the adsorption sites on the surface of iron oxide and react competitively for hydroxyl radicals, and thus might inhibit the photodegradation of organic pollutants [38]. Liu et al. [26] reported that 1.0 mM should be the optimal initial concentration of oxalic acid for photodegradation of 2-mercaptobenzothiazole by iron oxides in aqueous phase. The molar ratio of oxalate and iron oxide in aqueous phase was 0.22 when oxalate concentration was 1.0 mM [26]. In aqueous phase, the molar ratio of oxalate and iron oxide was over 0.22, the photodegradation rate decreased. In contrast, the photodegradation rate increased gradually with the increase in the molar ratio of oxalate and goethite from 0 to 1.34 in this study. When the molar ratio of oxalate and iron oxide in aqueous phase was 0.22, the total dissolved Fe^{2+} and Fe^{3+} was up to 25 mg/L in aqueous phase, while that was below 5 mg/L in solid media. Lower amount of dissolved Fe^{2+} and Fe^{3+} formation implies lower reaction efficiency between iron oxide and oxalate. This difference should also be attributed to the obstruction in the penetration of UV light in the solid phase.

3.6. Photodegradation products

The chromatogram picture of intermediate compound, pyreno, of this experiment is shown in Fig. 6. In order to further confirm this compound is pyreno, the analysis of intermediate compound was conducted. The result confirmed that it was pyreno with 72% possibility (Fig. 7). Therefore, pyreno could be considered as the main intermediate product. Eibes et al. [39] had reported that 1-hydroxypyrene may be one of the intermediate compounds from enzymatic degradation of pyrene by manganese peroxidase in media containing acetone. However, 1-hydroxypyrene was not found in the present experiments. Zeng et al. [40] reported other degradation intermediate compounds of pyrene in ozonated water, including 2,2′,6,6′-biphenyltetraaldehyde,

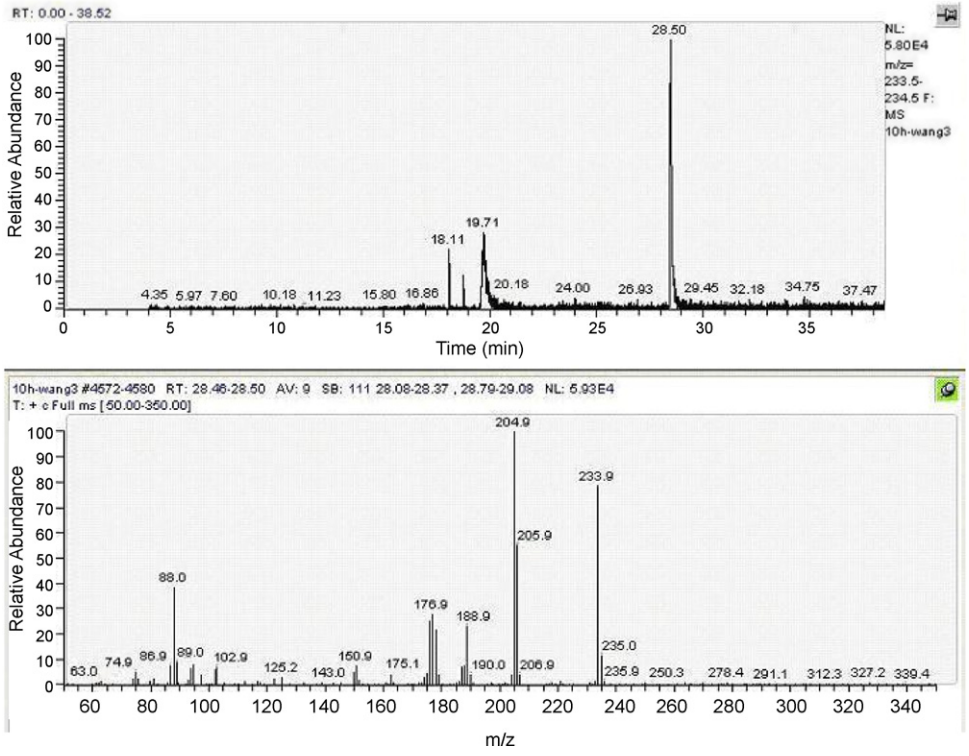

Fig. 6. Chromatogram picture of intermediate compound pyreno in the experiment.

4,5-phenanthrenedialde-hyde, 1,2-benzenedicarboxylic acid and diisooctyl. The difference in intermediate compounds might imply the different degradation pathway.

3.7. Photodegradation of PAHs in contaminated soil

Red soil collected in Southern China was used to test the degradation of PAHs in contaminated soil using similar procedure described above. Nine different types of PAHs were detected in the soil sample with their corresponding PAHs concentrations listed in Table 3. Prior to irradiation with the UV light intensity of 480 μW/cm^2, the soil sample was processed by adding 3.0 mL of 1.0 mM oxalic acid into 10 g of soil. The content of PAHs was detected by GC–MS [41,42] and the results are shown in Table 4. The results indicated that all the content of PAHs decreased after 12 h irradiation. The degradation percentages were 12.3, 13.6, 21.1, 12.2, 16.4, 20.0, 21.7, 17.9 and 21.8% for Fluoranthene, Pyrene, Benzo[*a*]anthracene, Chrysene, Benzo[*b*]fluoranthene, Benzo[*k*]fluoranthene, Benzo[*a*]pyrene, Indeno[1,2,3-*cd*]pyrene, and Benzo[*ghi*]perylene, respectively. It can be confirmed that PAHs should be effectively photodegraded in real soils.

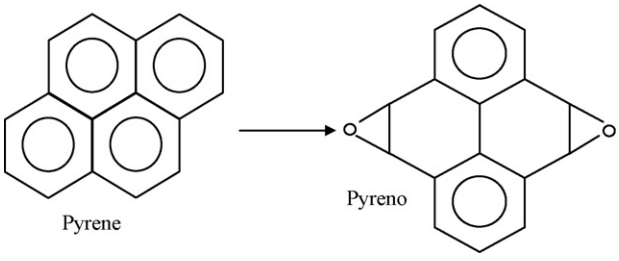

Fig. 7. Intermediate compounds from the degradation pyrene in experiments.

3.8. The mechanism of the pyrene photodegradation in solid phase

In absence of carboxylic acids, iron oxides can act as natural photocatalysts to catalyze degradation of organic pollutants in environment. The band gap (E_g) of α-FeOOH, γ-FeOOH, γ-Fe_2O_3 and α-Fe_2O_3 are 2.10, 2.06, 2.03 and 2.02 eV, respectively. When irradiated by UV light, electrons receive energy from the photons and are thus excited from VB to CB as in Eq. (1) [20,21].

$$\text{Iron oxides} + h\upsilon \rightarrow e^- + h^+ \quad (1)$$

After formation of electron–hole pair, the hydroxyl radicals (•OH) with higher redox potential can be generated by a series of reactions as Eqs. (2)–(6). And then PAHs could be oxidized by •OH as showed in Fig. 8(a).

$$H_2O + h^+ \rightarrow H^+ + {}^\bullet OH \quad (2)$$

$$O_2 + e^- \rightarrow {}^\bullet O_2{}^- \quad (3)$$

$${}^\bullet O_2{}^- + H^+ \rightarrow HOO^\bullet \quad (4)$$

Table 4
Photodegradation of PAHs in contaminated soil

PAHs	The concentration of PAH (mg/kg)		The degradation percentage (%)
	Initial	Irradiation after 12 h	
Fluoranthene	0.7147	0.6270	12.3
Pyrene	0.4823	0.4167	13.6
Benzo[*a*]anthracene	0.1952	0.1540	21.1
Chrysene	0.3532	0.3102	12.2
Benzo[*b*]fluoranthene	0.3977	0.3326	16.4
Benzo[*k*]fluoranthene	0.0927	0.0742	20.0
Benzo[*a*]pyrene	0.1586	0.1242	21.7
Indeno[1,2,3-*cd*]pyrene	0.1814	0.1490	17.9
Benzo[*ghi*]perylene	0.1939	0.1517	21.8

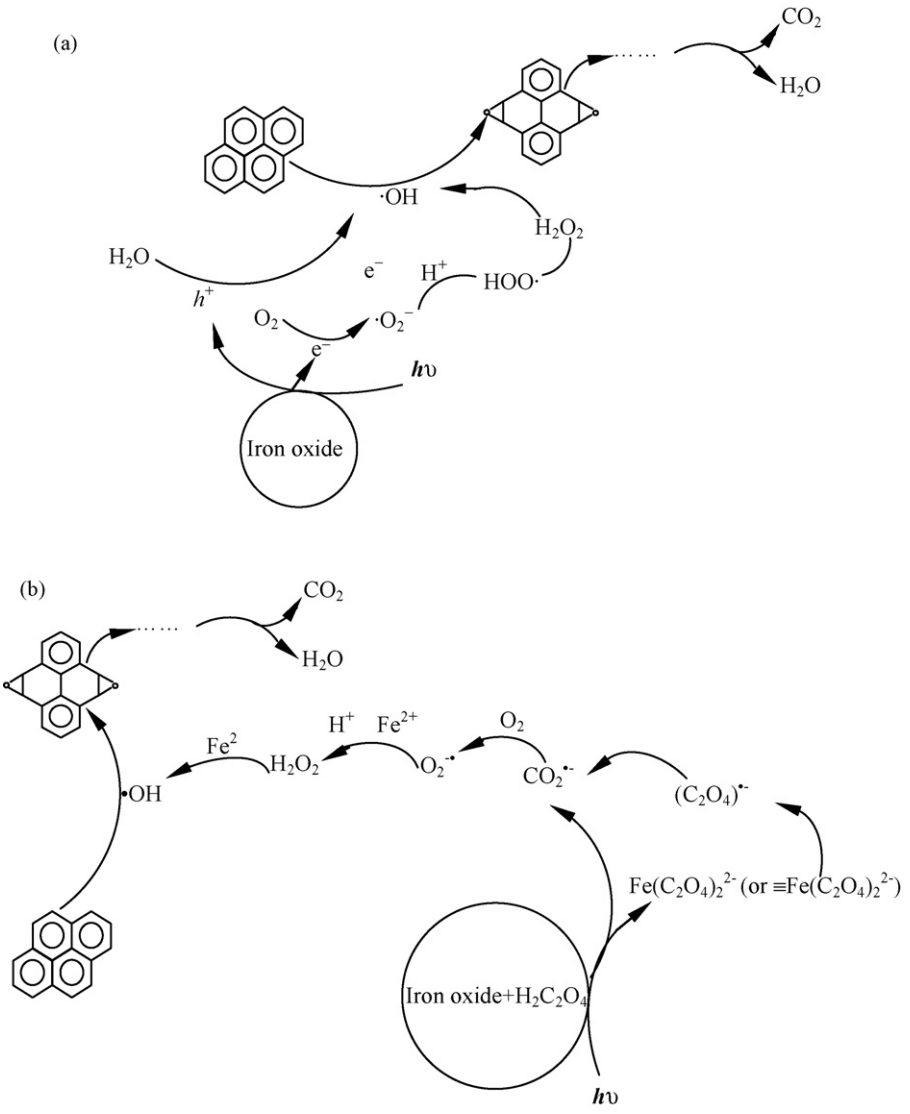

Fig. 8. The mechanism of the pyrene photodegradation in solid phase.

$$2HOO^{\bullet} \rightarrow H_2O_2 + O_2 \quad (5)$$

$$H_2O_2 + e^- \rightarrow OH^- + {}^{\bullet}OH \quad (6)$$

$$PAHs + {}^{\bullet}OH \rightarrow degradationproducts \quad (7)$$

In presence of oxalic acid, iron oxide together with oxalic acid set up a Fenton-like system. The principle of the reaction can be described as Eqs. (8)–(12) and in Fig. 8(b) [24,26].

$$[\equiv Fe(C_2O_4)_n]^{(2n-3)-} + h\nu \rightarrow Fe(C_2O_4)_2{}^{2-} (or \equiv Fe(C_2O_4)_2{}^{2-}) + CO_2{}^{\bullet -} \quad (8)$$

$$(C_2O_4)^{\bullet -} \rightarrow CO_2 + CO_2{}^{\bullet -} \quad (9)$$

$$CO_2{}^{\bullet -} + O_2 \rightarrow CO_2 + O_2{}^{-\bullet} \quad (10)$$

$$O_2{}^{-\bullet} + nH^+ + Fe^{2+} \rightarrow Fe^{3+} + H_2O_2 \quad (11)$$

$$Fe^{2+} + H_2O_2 \rightarrow Fe^{3+} + OH^- + {}^{\bullet}OH \quad (12)$$

Although the photochemical mechanism in solid media should almost be the same as that in aqueous phase, the effect of influencing factors on the photodegradation of organic pollutants is different. In solid media, the low penetration rate of UV light resulted in the lower enhancement effect of light intensity and additional oxalate on pyrene photodegradation.

4. Conclusions

Results of the present work suggest that the photodegradation of pyrene in solid phase depended on the type of iron oxide, the dosage of iron oxides, initial concentration of oxalic acid and intensity of UV light. An intermediate compound, pyreno was detected during the process of pyrene photodegradation. PAHs degradation by photo-Fenton-like system could occur in real soil and the degradation rates of the 9 PAHs present in the contaminated soil were between 12.2 and 21.8% in the presence of oxalic acid after 12 h irradiation with the light intensity of 480 $\mu W/cm^2$. This work provides useful information to develop the photochemical remediation techniques of PAHs contaminated soils in a more realistic condition.

Acknowledgments

This work was supported by the China National Natural Science Foundation Project No. 20577007 and Guangdong Natural Science Foundation Key Project No. 036533.

References

[1] J. Jacob, The significance of polycyclic aromatic hydrocarbons as environmental carcinogens, Pure Appl. Chem. 68 (1996) 301–308.
[2] C. Menzie, B.B. Potocki, J. Santodonato, Exposure to carcinogenic PAHs in the environment, Environ. Sci. Technol. 26 (1992) 1278–1284.
[3] P. Henner, M. Schiavon, J.L. Morel, E. Lichtfouse, Polycyclic aromatic hydrocarbon (PAH) occurrence and remediation methods, Anal. Mag. 25 (1997) 56–59.
[4] S.K. Ssamantha, A.K. Chakrabori, R.K. Jain, Degradation of phenanthrene by different bacteria: evidence for novel transformation sequence involving the formation of 1-naphthol, Appl. Microbial. Biotechnol. 53 (1999) 98–107.
[5] K. Nam, J.J. Kukor, Combined ozonation and biodegradation for remediation of mixtures of polycyclic aromatic hydrocarbons in soil, Biodegradation 11 (2000) 1–9.
[6] K.M. Lehto, J.A. Puhakka, H. Lemmetyinen, Biodegradation of selected UV-irradiated and non-irradiated polycyclic aromatic hydrocarbons, Biodegradation 14 (2003) 249–263.
[7] N.N. Pozdnyakova, J. Rodakiewicz-Nowak, O.V. Turkovskaya, J. Haber, Oxidative degradation of polyaromatic hydrocarbons and their derivatives catalyzed directly by the yellow laccase from *pleurotus osreatus* D1, J. Mol. Catal. B 41 (2006) 8–15.
[8] X.J. Li, P.J. Li, X. Lin, C.G. Zhang, Q. Li, Z.Q. Gong, Biodegradation of aged polycyclic aromatic hydrocarbons (PAHs) by microbial consortia in soil and slurry phases, J. Hazard. Mater. 150 (2008) 21–26.
[9] A. Masih, A. Taneja, Polycyclic aromatic hydrocarbons (PAHs) concentrations and related carcinogenic potencies in soil at a semi-arid region of India, Chemosphere 65 (2006) 449–456.
[10] S.K. Samanta, O.V. Singh, P.K. Jain, Polycyclic aromatic hydrocarbons: environmental pollution and bioremediation, Trends Biotechnol. 20 (2002) 243–248.
[11] S. Kohtani, M. Tomohiro, K. Tokumura, R. Nakagaki, Photooxidation reactions of polycyclic aromatic hydrocarbons over pure and Ag-loaded $BiVO_4$ photocatalysts, Appl. Catal. B 58 (2005) 265–272.
[12] M.R. Hoffmann, S.T. Martin, W. Choi, D.W. Bahnemann, Environmental applications of semiconductor photocatalysis, Chem. Rev. 95 (1995) 69–96.
[13] A. Fujishima, K. Hashimoto, T. Watanabe, TiO_2 Photocatalysis Fundamental and Application, BKC, Tokyo, 1999.
[14] D.S. Bhatkhande, V.G. Pangarkar, A.A.C.M. Beenackers, Photocatalytic degradation for environmental applications—a review, J. Chem. Technol. Biotechnol. 77 (2001) 102–116.
[15] M.E. Sigman, P.F. Schuler, M.M. Ghosh, R.T. Dabestani, Mechanism of pyrene photochemical oxidation in aqueous and surfactant solutions, Environ. Sci. Technol. 32 (1998) 3980–3985.
[16] S. Wen, J. Zhao, G. Shen, J. Fu, P. Peng, Photocatalytic reactions of pyrene at TiO_2/water interfaces, Chemosphere 50 (2003) 111–119.
[17] S. Jonsson, Y. Persson, S. Frankki, B.V. Bavel, S. Lundstedt, P. Haglund, M. Tysklind, Degradation of polycyclic aromatic hydrocarbons (PAHs) in contaminated soils by Fenton's reagent: a multivariate evaluation of the importance of soil characteristics and PAH properties, J. Hazard. Mater. 149 (2007) 86–96.
[18] H.F. Lin, K.T. Valsaraj, A titania thin film annular photocatalytic reactor for the degradation of polycyclic aromatic hydrocarbons in dilute water streams, J. Hazard. Mater. 99 (2003) 203–219.
[19] U. Schwertmann, R.M. Cornell, Iron Oxides in the Laboratory: Preparation and Characterization, VCH, New York, 1991.
[20] J.K. Leland, A.J. Bard, Photochemistry of colloidal semiconducting iron oxide polymorphs, J. Phys. Chem. 91 (1987) 5076–5083.
[21] F.B. Li, X.Z. Li, C.S. Liu, T.X. Liu, Effect of alumina on photocatalytic activity of iron oxides for bisphenol A degradation, J. Hazard. Mater. 149 (2007) 199–207.
[22] T. Kayashima, T. Katayama, Oxalic acid is available as a natural antioxidant in some systems, Biochim. Biophys. Acta—Gen. Subjects 1573 (2002) 1–3.
[23] C. Siffert, B. Sulzberger, Light-induced dissolution of hematite in the presence of oxalate: a case study, Langmuir 7 (1991) 1627–1634.
[24] B.C. Faust, J. Allen, Photochemistry of aqueous iron(III)-polycarboxylate complexes: roles in the chemistry of atmospheric and surface waters, Environ. Sci. Technol. 27 (1993) 2517–2522.
[25] F.S. Yen, W.Ch. Chen, J.M. Yang, Ch.T. Hong, Crystallite size variations of nanosized Fe_2O_3 powders during γ- to α-phase transformation, Nano Lett. 2 (2002) 245–252.
[26] C.S. Liu, F.B. Li, X.M. Li, G. Zhang, Y.Q. Kuang, The effect of iron oxides and oxalate on the photodegradation of 2-mercaptobenzothiazole, J. Mol. Catal. A 252 (2006) 40–48.
[27] Joint Committee for Powder Diffraction Standards, "JCPDS" International Center for Diffraction Data, 1979.
[28] J.G. Yu, J.C. Yu, M.K.P. Leung, W.K. Ho, B. Cheng, X.J. Zhao, J.C. Zhao, Effects of acidic and basic hydrolysis catalysts on the photocatalytic activity and microstructures of bimodal mesoporous titania, J. Catal. 217 (2003) 69–78.
[29] Y. Yu, J.C. Yu, J.G. Yu, Y.C. Kwok, Y.K. Che, J.C. Zhao, L. Ding, W.K. Ge, P.K. Wong, Enhancement of photocatalytic activity of mesoporous TiO_2 by using carbon nanotubes, Appl. Catal. A 289 (2005) 186–196.
[30] G.Q. Song, C. Lu, J.M. Lin, Application of surfactants and microemulsions to the extraction of pyrene and phenanthrene from soil with different extraction methods, Anal. Chim. Acta 596 (2007) 312–318.
[31] E. Sepetdjian, A. Shihadeh, N.A. Saliba, Measurement of 16 polycyclic aromatic hydrocarbons in narghile waterpipe tobacco smoke, Food Chem. Toxicol. 46 (2008) 1582–1590.
[32] C. Ravelet, C. Grosset, B. Montuelle, J.L. Benoit-Guyod, J. Alary, Liquid chromatography study of pyrene degradation by two micromycetes in a freshwater sediment, Chemosphere 44 (2001) 1541–1546.
[33] J.F. Niu, J.W. Chen, D. Martens, X. Quan, F.L. Yang, A. Kettrup, K.W. Schramm, Photolysis of polycyclic aromatic hydrocarbons adsorbed on spruce [*Picea abies* (L.) Karst.] needles under sunlight irradiation, Environ. Pollut. 123 (2003) 39–45.
[34] R.M. Cornell, U. Schwertmann, The Iron Oxides-Structure, Properties, Reactions, Occurrences and Uses, second ed., Druckhaus Darmstadt, Darmstadt, 2003.
[35] J. Guo, Y. Luo, Y.L. Chen, X.T. Bao, L.A. Chong, Study on photochemical degradation of polycyclic aromatic hydrocarbons (PAHs) from coal-fired flue gas, Energy Environ. Prot. 20 (2006) 25–28 (In Chinese).
[36] M.H. Zhou, J.G. Yu, B. Cheng, Effects of Fe-doping on the photocatalytic activity of mesoporous TiO_2 powders prepared by an ultrasonic method, J. Hazard. Mater. B137 (2006) 1838–1847.
[37] Y.G. Zuo, Y.W. Deng, Iron(II)-catalyzed photochemical decomposition of oxalic acid and generation of H_2O_2 in atmospheric liquid phases, Chemosphere 35 (1997) 2051–2058.
[38] J. Lei, C.S. Liu, F.B. Li, X.M. Li, S.G. Zhou, T.X. Liu, M.H. Gu, Q.T. Wu, Photodegradation of orange I in the heterogeneous iron oxide–oxalate complex system under UVA irradiation, J. Hazard. Mater. 37 (2006) 1016–1024.
[39] G. Eibes, T. Cajthaml, M.T. Moreira, G. Feijoo, J.M. Lema, Enzymatic degradation of anthracene, dibenzothiophene and pyrene by manganese peroxidase in media containing acetone, Chemosphere 64 (2006) 408–414.
[40] Y. Zeng, P.K.A. Hong, D.A. Wavrek, Chemical-biological treatment of pyrene, Water Res. 34 (2000) 1157–1172.
[41] B.X. Mai, J.M. Fu, G.Y. Sheng, Y.H. Kang, Z. Lin, G. Zhang, Y.S. Min, E.Y. Zeng, Chlorinated and polycyclic aromatic hydrocarbons in riverine and estuarine sediments from Pearl River Delta, China, Environ. Pollut. 117 (2002) 457–474.
[42] J. Li, G. Zhang, X.D. Li, S.H. Qi, G.Q. Liu, X.Z. Peng, Source seasonality of polycyclic aromatic hydrocarbons (PAHs) in a subtropical city, Guangzhou, South China, Sci. Total Environ. 355 (2006) 145–155.